IEEE Access
Multidisciplinary | Rapid Review | Open Access Journal

Received December 26, 2017, accepted January 23, 2018, date of publication February 8, 2018, date of current version March 16, 2018.

Digital Object Identifier 10.1109/ACCESS.2018.2803745

Practical Design of a Speaker Box With a Passive Vibrator (February 2018)

HYUNG-KYU KIM[1], YUAN-WU JIANG[1], DAN-PING XU[1,2], JOONG-HAK KWON[3], AND SANG-MOON HWANG[1]

[1]School of Mechanical Engineering, Pusan National University, Busan 609-735, South Korea
[2]School of Mechanical Engineering and Automation, Shanghai University, Shanghai 200072, China
[3]Research and Development Center, EM-Tech, Changwon 642-120, South Korea

Corresponding author: Sang-Moon Hwang (shwang@pusan.ac.kr)

ABSTRACT With the rapid development of multimedia devices, such as smart phones and tablet PCs, and wearable devices such as neckband speakers are being used increasingly as audio equipment. Typically, one side of a neckband speaker consists of a microspeaker driver integrated in a speaker box and a linear vibrator independent of the speaker box. In this paper, a practical design of a passive radiator integrated in the speaker box is proposed as a substitute for the linear vibrator. Therefore, both of the microspeaker driver and the passive vibrator are integrated in the speaker box. 2-DOF theory is used to model the system, and parameters are identified using Klippel and the analytical method. The sound pressure is obtained by the boundary element method. First, the prototype of a passive vibrator is built by using a center diaphragm and a side diaphragm. Then, the parameters of the prototypes are determined. An acceleration test is conducted to check the vibrator performance. Finally, an optimized vibrator is manufactured by using the analytical method. The sound pressure level (SPL) and acceleration are determined and conduct a response time experiment. The results show that the SPL values obtained through both of the experiment and simulation show good agreement and that there is only 2 dB sacrificed owing to the passive vibrator. The acceleration experiment results show that the optimized passive vibrator can generate 1.5 Grms at 130 Hz; this represents an improvement of 60% compared with the prototype. Furthermore, the response time of the passive vibrator is 20 ms. The proposed passive vibrator can be used to develop commercial neckband speakers.

INDEX TERMS Passive vibrator, speaker box, sound pressure level, acceleration.

I. INTRODUCTION

Wearable electronic devices such as neckband speakers are becoming increasingly popular because of the convenience they offer. One side of a typical neckband speaker consists of a microspeaker integrated in a speaker box and a linear vibrator independent of the speaker box, as shown in Fig. 1. When the microspeaker is working, a linear vibrator can generate low-frequency vibrations whose low bandwidth enables users to play music while engaged in some activity. However, a neckband speaker with a linear vibrator is expensive and cannot have a compact design. Therefore, a passive vibrator integrated in the speaker box is used to substitute for the linear vibrator to solve these two problems.

Vibrators in modern devices need to be highly responsive. Nam *et al*. [1] developed a linear vibrator with a fast response time. Park *et al*. [2] designed and optimized the structure of the linear vibrator used in touchscreen mobile phones. Another study investigated the back volume of the speaker box when designing the microspeaker unit [3]. Olson applied a passive radiator to a speaker system [4]. Small analyzed a speaker system with a passive radiator by using the equivalent circuit method [5]. Jiang developed a microspeaker system with a passive radiator structure by using two degrees of freedom (DOFs) to enhance the sound pressure level (SPL) from 150 to 500 Hz [6].

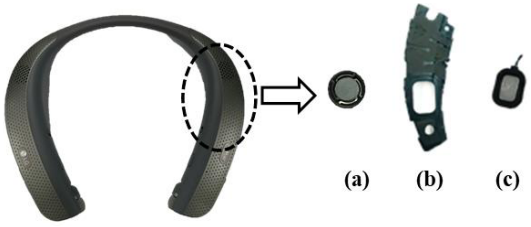

FIGURE 1. A typical neckband speaker (a) Linear vibrator, (b) speaker box, and (c) microspeaker driver.

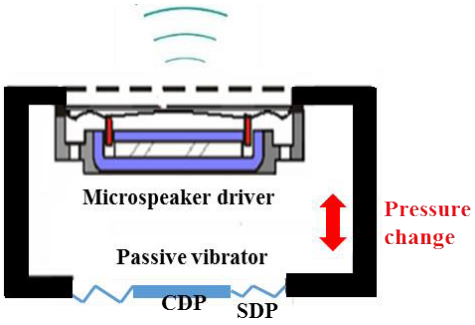

FIGURE 2. Sectional-view of the speaker box with a passive vibrator.

In this study, a passive vibrator is used to generate vibrations. An analytical method was used and verified experimentally. Based on the analytical method, an improved vibrator was manufactured to enhance the acceleration.

II. MODELING

Fig. 2 shows the working principle of a passive vibrator with a speaker box in sectional-view. With an input current, a coil will vibrate owing to the Lorenz force. As a result, the coil causes the diaphragm to vibrate, thereby producing a sound in front of the microspeaker driver. Simultaneously, the pressure change produces vibrations in the passive vibrator. Ultimately, sound pressure and vibration are both generated in one speaker box system. This can be modeled as a 2-DOF vibration system, as shown in Fig. 3.

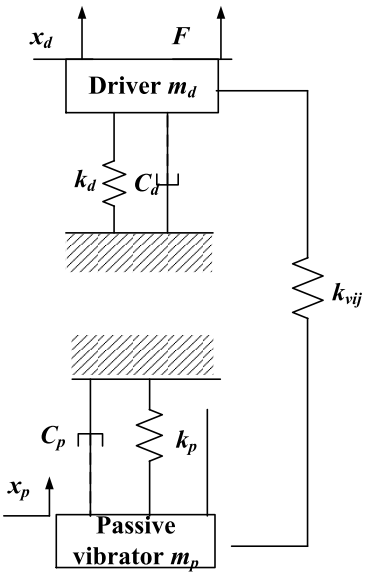

FIGURE 3. The schematic diagram of the speaker box with a passive vibrator in 2-DOF vibration system.

The governing equation of the modeled 2-DOF vibration system is

$$m_d\ddot{x}_d + k_d x_d + C_d\dot{x}_d + \frac{\rho_0 c^2 S_d^2}{V_{cc}}x_d - \frac{\rho_0 c^2 S_d S_p}{V_{cc}}x_p = Fe^{jwt}a$$
$$m_p\ddot{x}_p + k_p x_p + C_p\dot{x}_p + \frac{\rho_0 c^2 S_p^2}{V_{cc}}x_p - \frac{\rho_0 c^2 S_d S_p}{V_{cc}}x_d = 0 \quad (1)$$

where

$$x_d = |x_d|\, e^{jwt+\theta_d}, \quad x_p = |x_p|\, e^{jwt+\theta_p}$$

In Eq. (1), m_d, k_d, C_d, S_d, and x_d denote the mass, stiffness, damping, effective area, and displacement of the vibration part of the microspeaker microspeaker driver, and m_p, k_p, C_p, S_p, and x_p denote the corresponding values for the passive radiator. Furthermore, F, ρ_0, c, V_{cc}, and ω denote the Lorentz force, air density, air speed, back volume in speaker box, and angular frequency, respectively.

After solving the 2-DOF governing equation, the amplitude and phase of the displacement are obtained using Eq. (2). In Eq.(2), k_{vij} denotes the added stiffness caused by the back volume.

$$\begin{aligned} |x_d| &= \frac{F\sqrt{a_9^2 + a_{10}^2}}{a_7^2 + a_8^2} \\ \theta_d &= \tan^{-1}\left(\frac{a_{10}}{a_9}\right) \\ |x_p| &= \frac{F\,|a_4|\sqrt{a_7^2 + a_8^2}}{a_7^2 + a_8^2} \\ \theta_p &= \tan^{-1}\left(\frac{-a_8}{a_7}\right) \end{aligned} \quad (2)$$

where

$$\begin{aligned} a_1 &= -w^2 m_d + k_d + k_{v11} \\ a_2 &= wC_d \\ a_3 &= -k_{v12} \\ a_4 &= -k_{v21} \\ a_5 &= -w^2 m_p + k_p + k_{v22} \\ a_6 &= wC_p \\ a_7 &= a_1 a_5 - a_2 a_6 - a_3 a_4 \\ a_8 &= a_2 a_5 + a_1 a_6 \\ a_9 &= a_5 a_7 + a_6 a_8 \\ a_{10} &= a_6 a_7 - a_5 a_8 \\ k_{v11} &= \frac{\rho_0 c^2 S_d^2}{V_{cc}}, \quad k_{v12} = \frac{\rho_0 c^2 S_d S_p}{V_{cc}} \\ k_{v22} &= \frac{\rho_0 c^2 S_p^2}{V_{cc}}, \quad k_{v21} = \frac{\rho_0 c^2 S_d S_p}{V_{cc}} \end{aligned}$$

The displacement information can be treated as an input condition in boundary element method (BEM) modeling, as shown in Fig. 4. The boundary condition of the speaker box surface is that the normal velocity is zero, implying a rigid wall. With the given boundary and initial conditions, the velocity or sound pressure at every node can be obtained by surface modeling. Then, by using the boundary integral formula, the sound pressure at any point can be calculated [7]. The governing equation of BEM is the Helmholtz equation shown in Eq. (3). In Eq. (3), k and p denote the wave number and pressure respectively. The calculated point is set 0.1 m away from the speaker box.

$$\nabla^2 p + k^2 p = 0 \quad (3)$$

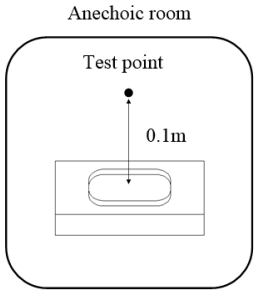

FIGURE 4. BEM modeling of the speaker box.

TABLE 1. Characteristics of the microspeaker driver.

Total width	20 mm
Total depth	15 mm
Total height	3.9 mm
DC resistance	6.16 Ω
Rater power	0.6 W

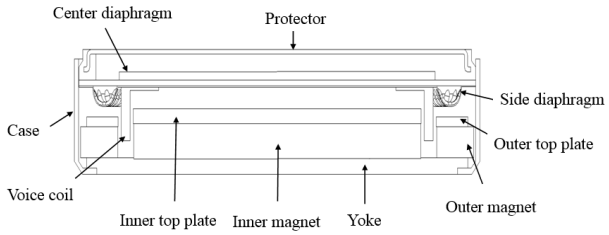

FIGURE 5. Structure of the microspeaker driver.

III. MANUFACTURING OF PROTOTYPE

A microspeaker driver and a passive vibrator are integrated in the speaker box, and the passive vibrator consists of a center diaphragm (CDP), and a side diaphragm (SDP).

Fig. 5 shows a cross-sectional view of a microspeaker driver, and Table 1 shows the characteristics of the microspeaker driver. The microspeaker driver has two permanent magnets, a yoke, an SDP, a CDP, a voice coil, two top plates, a protector, and a case. Fig. 6 shows the CDP and SDP of passive vibrator. Tables 2 and 3 separately show details about the CDP and SDP of the passive vibrator, and this is set as the prototype of passive vibrator. A tungsten CDP is attached at the center of the SDP. Fig. 7 shows the assembly sample of the speaker box with the prototype passive vibrator and the microspeaker driver after assembly.

IV. PARAMETER IDENTIFICATION

Fig. 8 shows a flowchart of the parameter identification procedures for the passive vibrator. First, the microspeaker driver parameters are identified using Klippel. Next, the passive vibrator's parameters were identified using the analytical method.

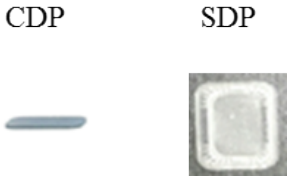

FIGURE 6. SDP and CDP in the passive vibrator.

TABLE 2. Details of CDP in the prototype passive vibrator.

Thickness mm)	Weight (g)	Material
0.5	0.78	Tungsten

TABLE 3. Details of SDP in the prototype passive vibrator.

Material
Polyetherether ketone + acrylic + polyetherether ketone 12 μm + 30 μm + 12 μm

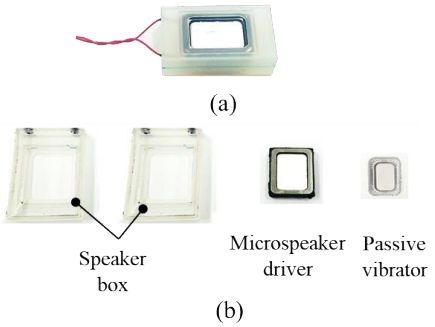

FIGURE 7. Sample and parts (a) Assembly sample and (b) component parts.

A. MICROSPEAKER DRIVER PARAMETER IDENTIFICATION

The T/S parameters of the microspeaker driver, such as mass, stiffness, damping, and force factor, were identified using Klippel [8]. As shown in Fig. 9, a 2.5 cm^3 box with a microspeaker driver is used to obtain the T/S parameters. Klippel was used to measure the T/S parameters of the driver and displacement of the passive vibrator, as shown in Fig. 10.

This module assumes that all parameters of the lumped elements are independent of the state variables. Table 4 shows the definitions of the T/S parameters identified using Klippel [8].

The electrical parameters are determined by calculating the voltage and current spectra. According to Klippel, the electrical parameters and impedance are related as follows [8]:

$$Z(f) = \frac{U(f)}{I(f)} = \frac{fL_{CES}}{f^2 L_{CES} C_{MES} + f\frac{L_{CES}}{R_{ES}} + 1} + \frac{fL_2 R_2}{fL_2 + R_2} + fL_E + R_E \quad (4)$$

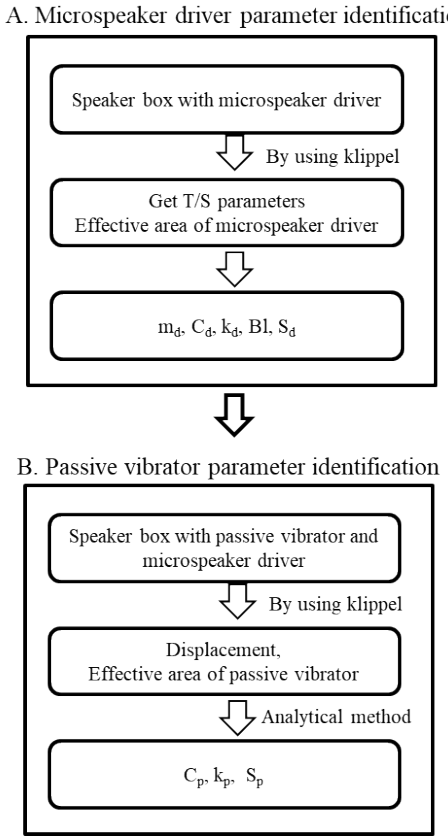

FIGURE 8. Flowchart of parameter identification.

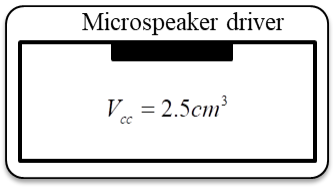

FIGURE 9. Speaker box with microspeaker driver (volume: 2.5 cm^3).

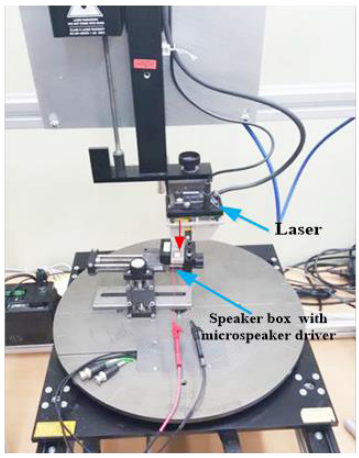

FIGURE 10. Schematic of experimental setup.

The estimated curve is obtained by least-squares fitting of the measured impedances. The electrical parameters for the impedance can be determined using this calculation.

TABLE 4. Definitions of T/S parameters.

Electrical Parameters	
R_E	Electrical voice coil resistance at DC
L_E	Voice coil inductance at low frequencies
L_2	Parainductance at high frequencies
R_2	Resistance due to eddy currents
Derived Parameters	
$C_{MES} = m_d/B^2l^2$	Electrical capacitance representing mechanical mass
$L_{CES} = C_{MS}B^2l^2$	Electrical inductance representing mechanical compliance
$R_{ES} = B^2l^2/C_d$	Resistance due to mechanical losses
f_s	Driver resonance frequency
Mechanical Parameters	
m_d	Mechanical mass of driver diaphragm assembly including air load and voice coil
C_d	Mechanical resistance of total-driver losses
k_d	Mechanical stiffness of driver suspension
$C_{MS} = 1/K_d$	Mechanical compliance of driver suspension
Bl	Force factor

The mechanical parameters are determined by calculating the voltage and displacement spectra. The mechanical parameters and transfer function are related as follows [8]:

$$H_x(f) = \frac{X(f)}{U(f)} = \frac{X(f)Blf}{U(f)}\frac{1}{Blf} = \frac{Z_R}{Z_R + Z_P + fL_E + R_E}\frac{1}{Blf} \tag{5}$$

where

$$Z_R(f) = \frac{fL_{CES}}{f^2L_{CES}C_{MES} + f\frac{L_{CES}}{R_{ES}} + 1}$$

$$Z_P(f) = \frac{fL_2R_2}{fL_2 + R_2} + fL_E + R_E$$

As for the electrical parameters, the mechanical parameters in the transfer function are determined by a least-squares fitting. Finally, the parameters of microspeaker driver are obtained as shown in Table 5.

In Klippel, the diaphragm is considered to be a rigid piston [9], as shown in Fig. 11.

According to the same complex volume velocity, the effective area is calculated using Eq. (6):

$$\underline{S}_D(w) = \frac{\underline{V}(w)}{jw\underline{x}_{coil}(w)} = \frac{\int_{Sc}\underline{x}(w, r_c)dS}{\underline{x}_{coil}(w)} \tag{6}$$

where $\underline{x}(w, r_c)$ denotes the displacement of one point on the diaphragm; r_c, the distance between this point and the center

TABLE 5. Parameters of microspeaker driver.

m_d	226	mg
k_d	1170	N/m
C_d	0.30	Ns/m
Bl	1.36	N/A

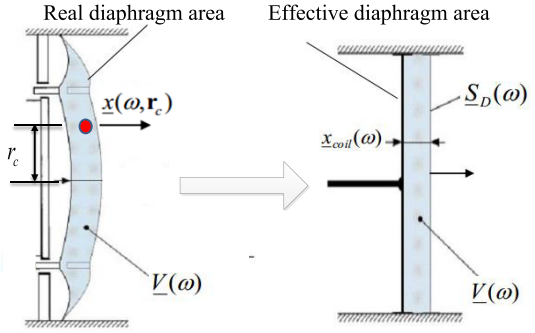

FIGURE 11. Effective area calculation method.

TABLE 6. Identification of the effective area.

Microspeaker driver			Passive vibrator		
S_d	189	mm^2	S_p	112	mm^2

point of the diaphragm; $\underline{V}(w)$, the complex volume velocity; $\underline{x}_{coil}(w)$, the average displacement of the point on the coil; and w, the angular frequency. Table 6 shows the experimentally obtained parameters.

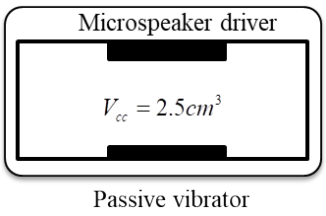

FIGURE 12. Speaker box with passive vibrator (volume: 2.5 cm3).

B. PASSIVE VIBRATOR PARAMETER IDENTIFICATION

The mass of the passive vibrator can be obtained by using an electronic scale (HR-200). In terms of the stiffness and damping of the passive vibrator, the T/S parameter is obtained by adjusting the parameter in the analytical method to match the experimental displacement obtained using Klippel. The tested frequency range is 50 −3000 Hz. A sweep sine signal is used for this purpose. As shown in Fig. 12, a 2.5 cm^3 box with a passive vibrator is used to obtain the experimental displacement.

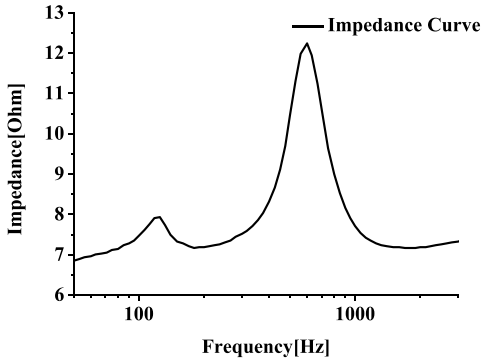

FIGURE 13. Experimental impedance curve obtained using Klippel.

The impedance curve shown in Fig. 13 is important to obtain the magnetic force.

The current curve is calculated from the experimental impedance curve. Then, the magnetic force is calculated by the following equation:

$$F = Bil \tag{7}$$

Fig. 14 shows a comparison of the displacement values obtained through the experiment and analysis for the microspeaker driver and passive vibrator. Table 7 shows the parameters of the passive vibrator. Table 8 lists the identified parameters of the prototype passive vibrator with a speaker box.

TABLE 7. Parameters of passive vibrator.

Passive vibrator		
m_p	820	mg
k_p	1400	N/m
C_p	0.32	N s/m

TABLE 8. Parameters of prototype passive vibrator with a speaker box.

Microspeaker driver			Passive vibrator		
m_d	226	mg	m_p	820	mg
k_d	1170	N/m	k_p	1400	N/m
C_d	0.30	Ns/m	C_p	0.32	N s/m
S_d	189	mm^2	S_p	112	mm^2

After the parameters are identified, an acceleration test is conducted to check the vibrator performance. Fig. 15 shows the acceleration test result of the prototype. The results reveal that the resonance frequency of the prototype is 230 Hz and the maximum acceleration is $0.9G_{rms}$. However, 230 Hz is

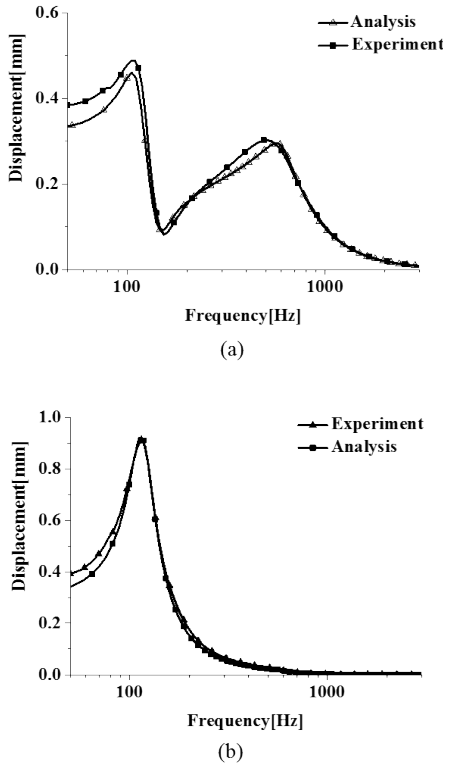

FIGURE 14. Comparison of displacement values obtained through experiment and analysis: (a) microspeaker driver and (b) passive vibrator.

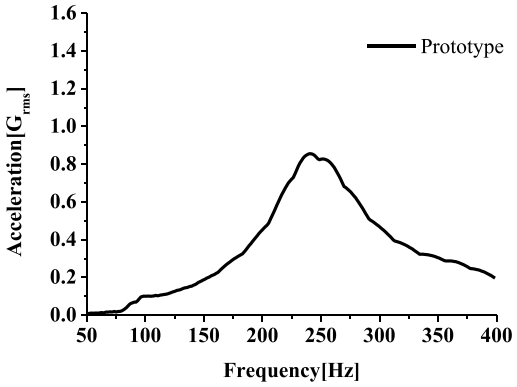

FIGURE 15. Experimental acceleration of prototype.

not a suitable frequency for the vibrator, and the acceleration is not enough for commercializing the product. Therefore, an improved passive vibrator is needed.

V. OPTIMIZATION OF VIBRATION

The damping is difficult to control. m_p, k_p are chosen as the parameters to be improved. Because the acceleration of the enclosure is proportional to the force of the passive vibrator, the objective function is defined as Eq. (8).

$$F_{vib} = m_p \ddot{x}_p \tag{8}$$

The optimization is conducted within the physically possible range, as shown in Table 9. Fig. 16 shows the optimization result. The results reveal that the force increases and the resonance frequency decreases when the mass of the passive vibrator increases and stiffness decreases.

TABLE 9. Parameter range for optimization.

	Prototype	Type 1	Type 2	
m_p	800	1200	1600	mg
k_p	1400	1200	1000	N/m

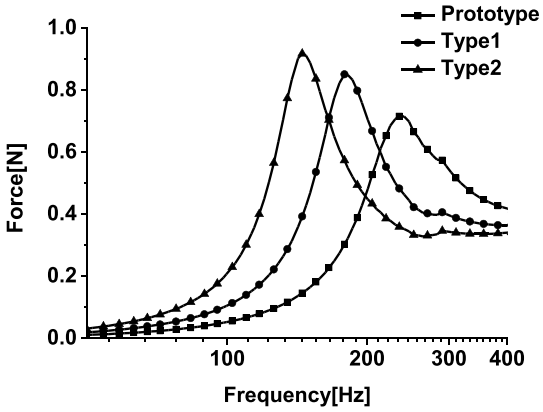

FIGURE 16. Analysis results of optimization.

TABLE 10. Detail of optimized passive vibrator.

CDP	Thickness [mm]	1
	Weight [g]	1.6
	Material	Tungsten
SDP	Thickness [mm]	70 μm + 30 μm + 70 μm
	Material	Thermoplastic polyurethane + acrylic + thermoplastic polyurethane

Finally, the optimized m_p, k_p values that maximize the objective function are selected as follows: $m_p = 1600$ mg and $k_p = 1000$ N/m. Table 10 shows details of the optimized vibrator.

VI. EXPERIMENT

A. ACOUSTIC PERFORMANCE TEST

A B&K Pulse system (3560C) was used for the acoustic performance experiment. To determine the influence of the passive vibrator on the SPL, two types of microspeaker systems were developed, as shown in Fig. 17. Fig. 18 shows an outline of the connections of the testing devices. The tested frequency range is 50 Hz to 20 kHz. A sweep sine signal is used. In the B&K system, the accepted sound signal is transformed to an SPL curve in the frequency domain by fast Fourier transform (FFT). The experiment is conducted in an anechoic room. The testing distance is selected as 0.1 m in the central axis direction.

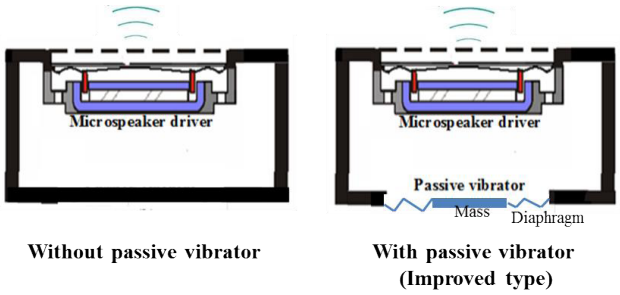

FIGURE 17. Two types of microspeaker system.

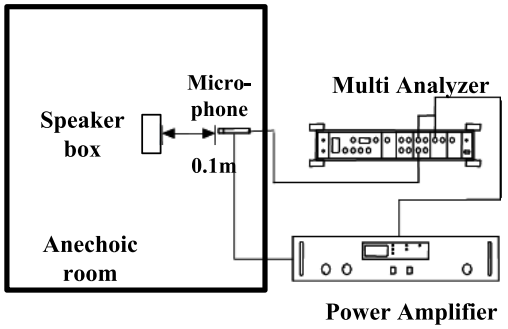

FIGURE 18. Experimental setup for SPL.

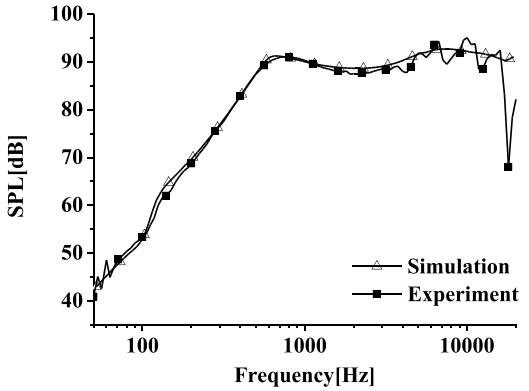

FIGURE 19. Comparison of SPL obtained through experiment and simulation.

Fig. 19 shows a comparison of the SPL obtained through the experiment and simulation. As shown in this figure, the values show good agreement in low frequency. However, above 3 kHz, the analysis results do not match the experiment results. The reason is that the 2-DOF vibration theory does not consider higher modes, and sound reflection is ignored. Fig. 20 shows a comparison of the SPL obtained through the experiment. As shown in this figure, the passive vibrator sacrifices 2dB in the 80–120 Hz range.

B. ACCELERATION AND RESPONSE TIME PERFORMANCE TEST

The most commonly used performance metric for a vibrator is the acceleration and response time. In the experiment,

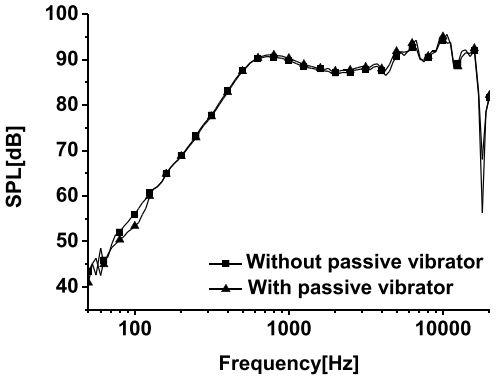

FIGURE 20. Influence of passive vibrator on SPL.

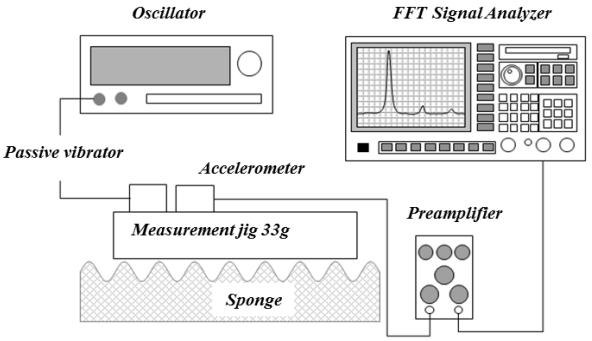

FIGURE 21. Test setup of acceleration experiment.

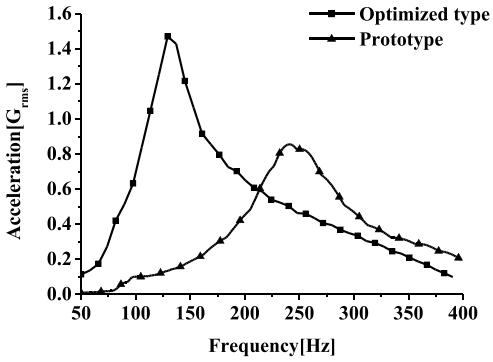

FIGURE 22. Acceleration experiment results.

a two-channel linear vibration motor tester (BK2120C) is used. Fig. 21 shows the test setup for the acceleration measurement. A 33g jig is used to fix the passive vibrator. The acceleration meter is attached to the jig. In the vibration motor tester, an acceleration meter is used to convert the mechanical strain into an electrical signal. The electronic circuit amplifies and transmits this signal to an external device. The response time of the passive vibrator was observed experimentally by measuring the acceleration of the vibration of the jig with the passive vibrator under a pure sine wave. For the acceleration test, the tested frequency range is 50–400 Hz. The final result is the curve in the frequency domain and time domain.

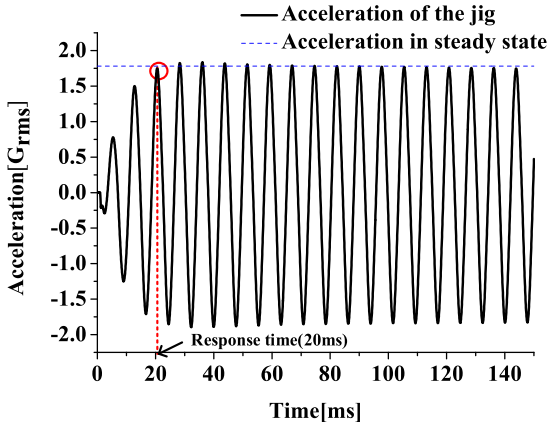

FIGURE 23. Measured response time of improved vibrator.

Fig. 22 shows an experiment result of the acceleration. The improved vibrator shows a resonance frequency of 130 Hz. The passive vibrator can generate an acceleration of 1.5 G_{rms}; this represents a 60% improvement in acceleration compared to the prototype. Fig. 23 shows the measured response time of the optimized vibrator. The acceleration of the optimized vibrator increases and repeats after 20 ms when the passive vibrator reaching the steady state of the vibration.

VII. CONCLUSION

Neckband speakers are being used increasingly because of the convenience they offer. One side of the neckband speaker usually consists of a microspeaker integrated in a speaker box and a linear vibrator independent of the speaker box. This study introduces a practical design of a speaker box with passive vibrator. A prototype of the passive vibrator is manufactured and tested with the speaker box. To build the prototype passive vibrator, a CDP and SDP are used. The 2-DOF vibration theory is used to model the system of a speaker box with passive vibrator. The analytical method is verified experimentally. Finally, the displacement and phase are identified using the analytical method. An acceleration test is conducted to check the vibrator performance. However, the resonance frequency of the prototype was not suitable and the acceleration is not enough for commercializing the product. Therefore, the optimized vibrator is manufactured within a physically possible range. The BEM is applied for SPL analysis. It is found that the SPL values obtained through the simulation and experiment show good agreement. Furthermore, 2dB SPL is sacrificed in the 80–120 Hz range owing to the passive vibrator. Finally, a vibration performance test is conducted. As shown in Fig. 22, the passive vibrator can generate 1.5G_{rms} at 130 Hz; this represents a 60% improvement compared to that of the prototype passive vibrator. Furthermore, the response time of the passive radiator is 20 ms; this is two times faster than that of the typical linear vibrator used in mobile phones [1]. Therefore, the proposed vibrator can react quickly when the microspeaker generates a sound. In conclusion, the proposed speaker box with passive vibrator can generate sound and vibration simultaneously. This practical design can be used to develop commercial neckband speakers. At the same time, space and cost can be saved by using this practical design.

REFERENCES

[1] J. Nam, T. Yeon, and G. Jang, "Development of a linear vibration motor with fast response time for mobile phones," *Microsyst. Technol.*, vol. 20, nos. 8–9, pp. 1505–1510, 2014.
[2] J. H. Park, P. Sun, J.-H. Kwon, and S.-M. Hwang, "Optimal design of linear vibrators used in touch screen mobile phones," *J. Mech. Sci. Technol.*, vol. 27, no. 2, pp. 313–318, 2013.
[3] D. P. Xu, P. Sun, J.-H. Kwon, and S.-M. Hwang, "An integrated design of microspeaker module with smaller volume," *J. Appl. Phys.*, vol. 115, no. 17, p. 17A339, 2014.
[4] H. F. Olson, "Loud speaker and method of propagating sound," U.S. Patent 1 988 250, Jan. 15, 1935.
[5] R. H. Small, "Passive-radiator loudspeaker systems Part 1: Analysis," *J. Audio Eng. Soc.*, vol. 22, no. 8, pp. 592–601, 1974.
[6] Y.-W. Jiang, J.-H. Kwon, H.-K. Kim, and S.-M. Hwang, "Analysis and optimization of speaker box using passive radiator," *Arch. Acoust.*, vol. 42, no. 4, pp. 753–760, 2017.
[7] P. K. Banerjee and R. Butterfield, *Boundary Element Methods in Engineering Science*. London, U.K.: McGraw-Hill, 1981.
[8] W. Klippel and U. Seidel, "Fast and accurate measurement of linear transducer parameters," in *Proc. 110th Audio Eng. Soc. Convention*, 2011.
[9] W. Klippel and J. Schlechter, "Dynamical measurement of the effective radiation area SD," in *Proc. 128th Audio Eng. Soc. Convention*, 2010.

HYUNG-KYU KIM received the B.S. degree from the School of Applied, Pusan National University, South Korea, where he is currently pursuing the M.S degree with the Laboratory of Vibration and Acoustic Design of Electro-Mechanical System of Mechanical Engineering. His interests are analysis, design, and optimization of passive speaker.

YUAN-WU JIANG received the M.S degree from the Laboratory of Vibration and Acoustic Design of Electro-Mechanical System of Mechanical Engineering from Pusan National University, South Korea, in 2016, where he is currently pursuing the Ph.D. degree. From 2014 to 2016, he was interested in the design, analysis, and optimization of passive speaker. Since 2017, his interests are the design and nonlinearity analysis of balanced armature receiver.

DAN-PING XU received the M.S. degree in electronic and information engineering from Chonbuk National University, South Korea, in 2012. She is currently pursuing the Ph.D. degree in mechanical engineering with Pusan National University, South Korea. From 2013 to 2014, she was interested in the field of the analysis, design, and optimization of moving-coil microspeaker and linear motor. Since 2015, her research interests include the design, nonlinearity analysis, and optimization of balanced armature receiver.

JOONG-HAK KWON received the M.S. and Ph.D. degrees from the Laboratory of Vibration and Acoustic Design of Electro-Mechanical System of Mechanical Engineering from Pusan National University, South Korea, in 2005 and 2009, respectively. He is currently the Head of Research and Development Department, EM-Tech. His interests include the design, analysis, and optimization of all electroacoustic products.

SANG-MOON HWANG received the M.S. and Ph.D. degrees in mechanical engineering from the University of California at Berkeley, Berkeley, CA, USA, in 1990 and 1994, respectively. He is currently a Professor in mechanical engineering with Pusan National University, South Korea. He is also CTO of EM-Tech, a Korean microspeaker company. His primary research interest is analysis, design, and optimization in microspeaker and linear vibrator.